DCC# T1300941-v1 **February 10, 2014**

LASER INTERFEROMETER GRAVITATIONAL WAVE OBSERVATORY

LIGO Laboratory / LIGO Scientific Collaboration

IO Mode Matching Diagnostics on the IOT Tables

R. Martin, P. Fulda, D. Feldbaum, C. Mueller, J. Gleason, L. Williams, G. Mueller, D. Tanner

Distribution of this document: LIGO Internal Collaboration
This is an internal working note of the LIGO Laboratory

California Institute of Technology
LIGO Project - MS 18-34
1200 E. California Blvd.
Pasadena, CA 91125
Phone (626) 395-2129
Fax (626) 304-9834
E-mail: info@ligo.caltech.edu

Massachusetts Institute of Technology
LIGO Project - NW22-295
185 Albany St.
Cambridge, MA 02139
Phone (617) 253-4824
Fax (617) 253-7014
E-mail: info@ligo.mit.edu

LIGO Hanford Observatory
P.O. Box 1970
Mail Stop S9-02
Richland, WA 99352
Phone (509) 372-8106
Fax (509) 372-8137

LIGO Livingston Observatory
P.O. Box 940
Livingston, LA 70754
Phone (225) 686-3100
Fax (225) 686-7189

http://www.ligo.caltech.edu/

I. PURPOSE AND SCOPE

This document describes the diagnostics and monitoring of the Input Optics mode matching on the IOT tables, using the as-built parameters available to date for L1 and H1. This document updates and replaces Sections 6, 7 and 8 of T0900407.

II. OPTICAL CONFIGURATION

The optical configuration for the Advanced LIGO interferometer is shown in Figure 1.The design parameters for all Advanced LIGO cavities are described in T0900043 and in T0900386.

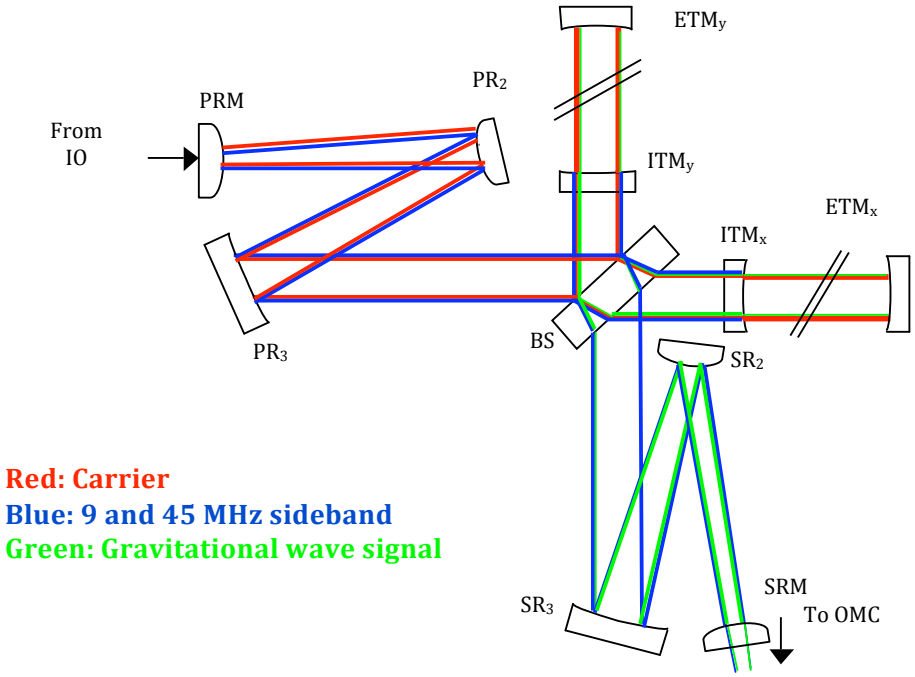

FIG. 1: Optical Layout of the Advanced LIGO Optical Cavities (*from T0900407-v4).*

The optical components responsible for the IO mode matching into the Power Recycling Cavity are shown in the conceptual optical layout in Figure 2. Two Pre-mode Matching telescope mirrors PMMT1 and PMMT2 shape the beam from the Input Mode Cleaner to match the beam size and radius of curvature at the Power Recycling Mirror.

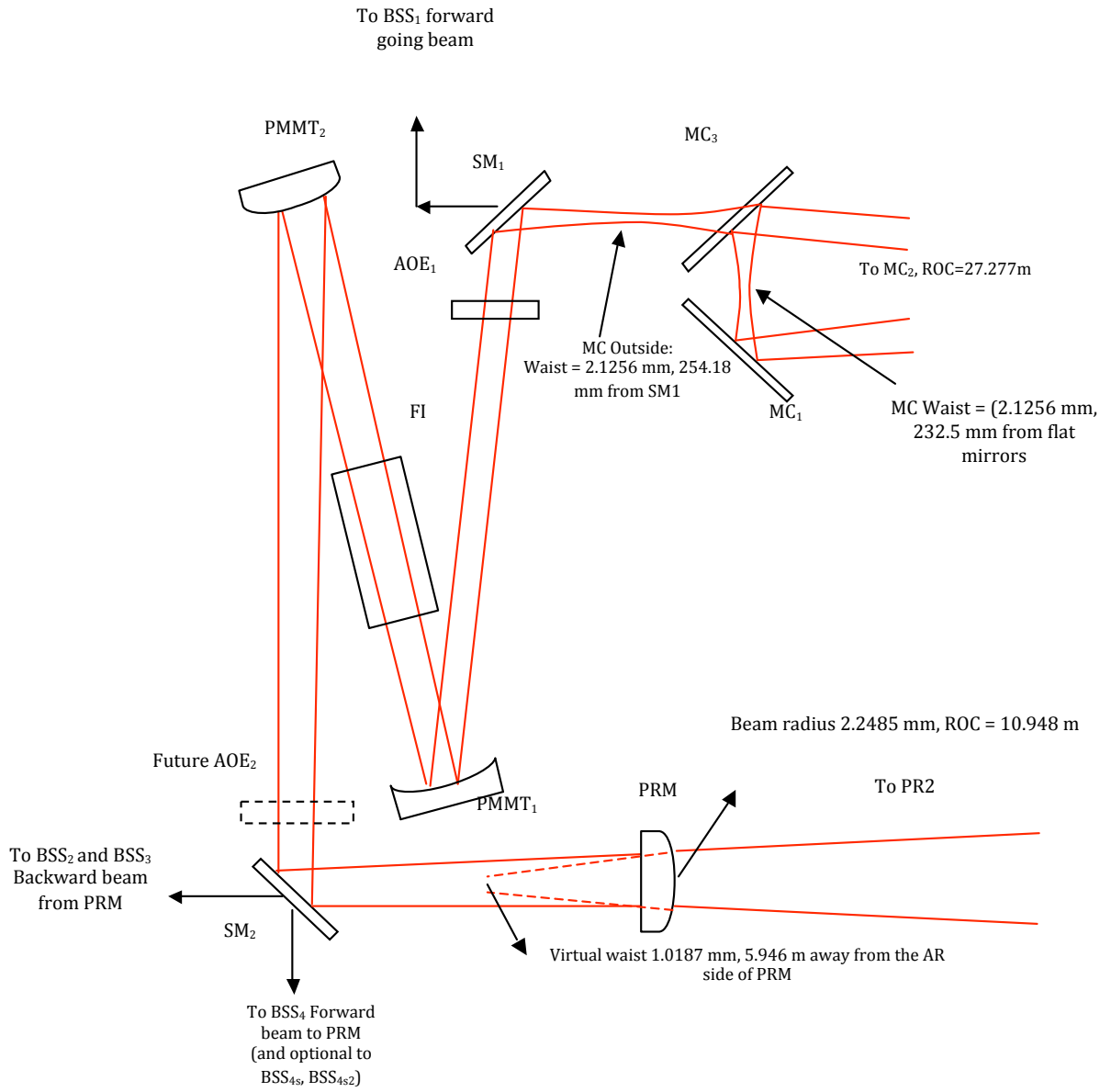

FIG. 2: Conceptual Layout of the Input Optics in HAM2 (*from T0900407-v4*). The values are derived for as-built parameters for H1.

A thorough discussion of the mode matching from the Input Mode Cleaner to the Power Recycling Cavity, including sources of mode mismatch and the effects of the fabrication and positioning tolerances of the PMMT mirrors, is given in the original document T0900407.

The as-built parameters and distances used in mode matching calculations are listed in TableI.

TABLE I: As-Built Parameters for L1 and H1 aLIGO Input Optics

Parameter	Unit	H1	Ref.	L1	Ref.
ROC of MC2 (H1: IMCC-02, L1: IMCC-03)	m	27.277	alog-8098	27.253	alog-5877
IMC Half Length	mm	16,473.5975	alog-5439	16,473.8238	alog-4702
Beam Size at MC2	mm	3.3775		3.3780	
Beam Waist Inside IMC	mm	2.1256		2.1244	
Location of IMC beam waist from MC1,3 HR	mm	232.5	E1200616-v7	232.5	E1200274-v3
Reduced Effective Thickness of MC3	mm	58.49		58.54	E1200339-v2
Reduced Effective Thickness of SM1	mm	20.71		20.71	
Location of IMC beam waist outside IMC from MC3-AR	mm	174.01		173.96	
Location of IMC beam waist from SM1-HR	mm	254.18		254.23	
Distance SM1 to PMMT1	mm	1,293.77	E1200616-v7	1,293.77	E1200274-v3
ROC of PMMT1	m	12.8	E080135-v2	12.8	E080135-v2
Beam Size at PMMT1	mm	2.1399		2.1387	
Distance PMMT1 to center of Faraday	mm	627.58	E1200616-v7	627.58	E1200274-v3
Beam Size at Faraday isolator	mm	1.9441		1.9431	
Distance from Center of Faraday to PMMT2	mm	542.73	E1200616-v7	542.73	E1200274-v3
ROC of PMMT2	m	-6.24	E080136-v2	-6.24	E080136-v2
Beam Size at PMMT2	mm	1.7797		1.7788	
Distance PMMT2 to SM2	mm	1,175.34	E1200616-v7	1,175.37	E1200274-v3
Distance SM2-HR to PRM-AR	mm	423.52	E1200616-v7	417.72	E1200274-v3
ROC of PRM (H1: PRM-04, L1: PRM-02)	m	10.948	T1300743-v1	11.009	T1300740-v1
Beam Size at PRM-HR	mm	2.2485		2.2489	
Beam Waist after PRM-AR	mm	1.0187		1.0203	
Beam Waist Location from PRM-AR (mode entering PRC)	m	5.946		5.986	
Reduced Effective Thickness of PRM	mm	50.91		51.00	E1200438-v1
Reduced Effective Thickness of SM2	mm	18.56		18.56	

Parameters in this table that have no reference listed in the adjacent column are derived values.

III. MODE MATCHING DIAGNOSTICS

The beam size and the Gouy phase evolution from the mode cleaner to the power recycling mirror is shown in Figure 3.

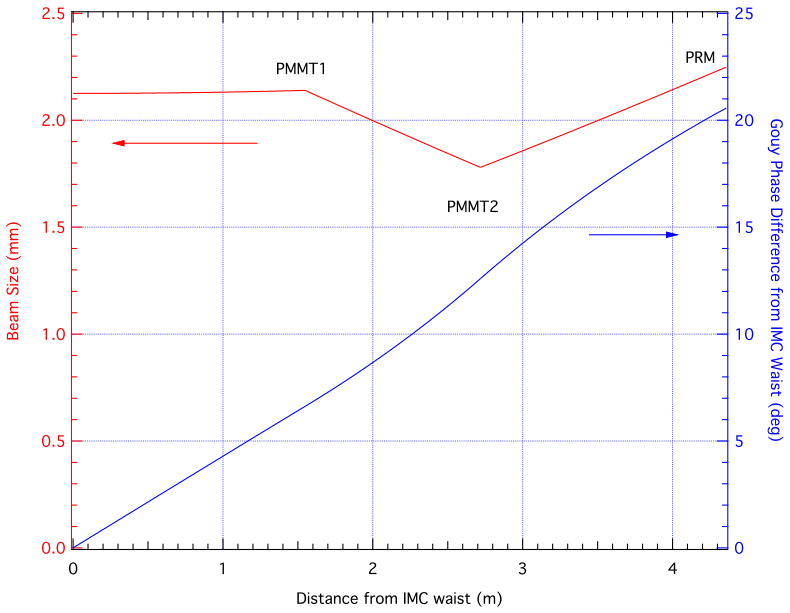

FIG. 3: Evolution of the beam size and accumulated Gouy phase from the waist of the mode cleaner to the power recycling mirror. These values are derived using the H1 as-built parameters. The beam parameters for L1 (listed in Table I) are very similar, and the evolution on the scale of this plot is identical.

To ensure that the beam provided at the PRM has the required beam size and radius of curvature, and to monitor the evolution of these parameters over time, we designed a set of Beam Size Sensors (BSS) to measure the profiles of beam samples at various locations on the Input Optics Tables IOT2L (previously known as IOT1) and IOT2R (pka IOT2).

These beams are:

- Beam entering the IFO after passing through the Input Optics *"IO Fwd through SM2"* - measured on IOT2R, after being transmitted through SM2 in forward propagation;
- Beam reflected off PRM (or returning from the arms) *"PRM Refl through SM2"* - measured on IOT2R, backward transmitted through SM2;

- Beam transmitted though the input mode cleaner *"MC Trans through SM1"* - measured on IOT2L after being transmitted through SM1;
- MC REFL beam - observed on IOT2L table, to check qualitatively the mode mismatch into the mode cleaner.

Table II summarizes the IO beam sensors and their purpose in monitoring the mode matching.

TABLE II: IO Beam Size Sensors on the IOT2L,R Tables

Sensor Name	Location	Purpose	IO Beam	Relationship with Monitored Value
BSS1	IOT2L (IOT1)	IMC Beam Size	MC Trans through SM1	Conjugate IMC beam waist *(180 deg Gouy phase from IMC waist)*
BSS2	IOT2R (IOT2)	PRM Beam Size	PRM Refl through SM2	Conjugate PRM beam size *(180 deg Gouy phase from PRM)*
BSS3	IOT2R (IOT2)	PRM Reflected	PRM Refl through SM2	Indirect ROC matching *(90 deg Gouy phase from PRM)*
BSS4	IOT2R (IOT2)	FI Thermal Lensing	IO Fwd through SM2	Indirect ROC matching *(90 deg Gouy phase from FI)*
BSS4s *(optional)*	IOT2R (IOT2)	FI Beam Size	IO Fwd through SM2	Conjugate FI beam size *(180 deg Gouy phase from FI)*
BSS4s2 *(optional)*	IOT2R (IOT2)	PRM Beam Size	IO Fwd through SM2	Conjugate PRM beam size *(180 deg Gouy phase from PRM)*
BSS5	IOT2L (IOT1)	IMC Reflected	PSL reflected off IMC1	Mode Mismatch into IMC

All BSS are aLIGO GigE cameras - Basler Ace 640-100gm, with 3.69 mm x 2.77 mm sensor size, and pixel size of 5.6 um. The location of the GigE cameras is shown in the IOT2L and IOT2R layouts LIGO-D0902284.

A diagram showing the positioning of these sensors on their beams w.r.t their pick-off optics (SM1 for the sensor in the MC Trans beam on IOT2L, and SM2 for the beams to IOT2R) is presented in Figure 4.

IV. MODE MATCHING ON IOT2L (IOT1)

There are two GigE cameras on the IOT2L table, BSS1 and BSS5.

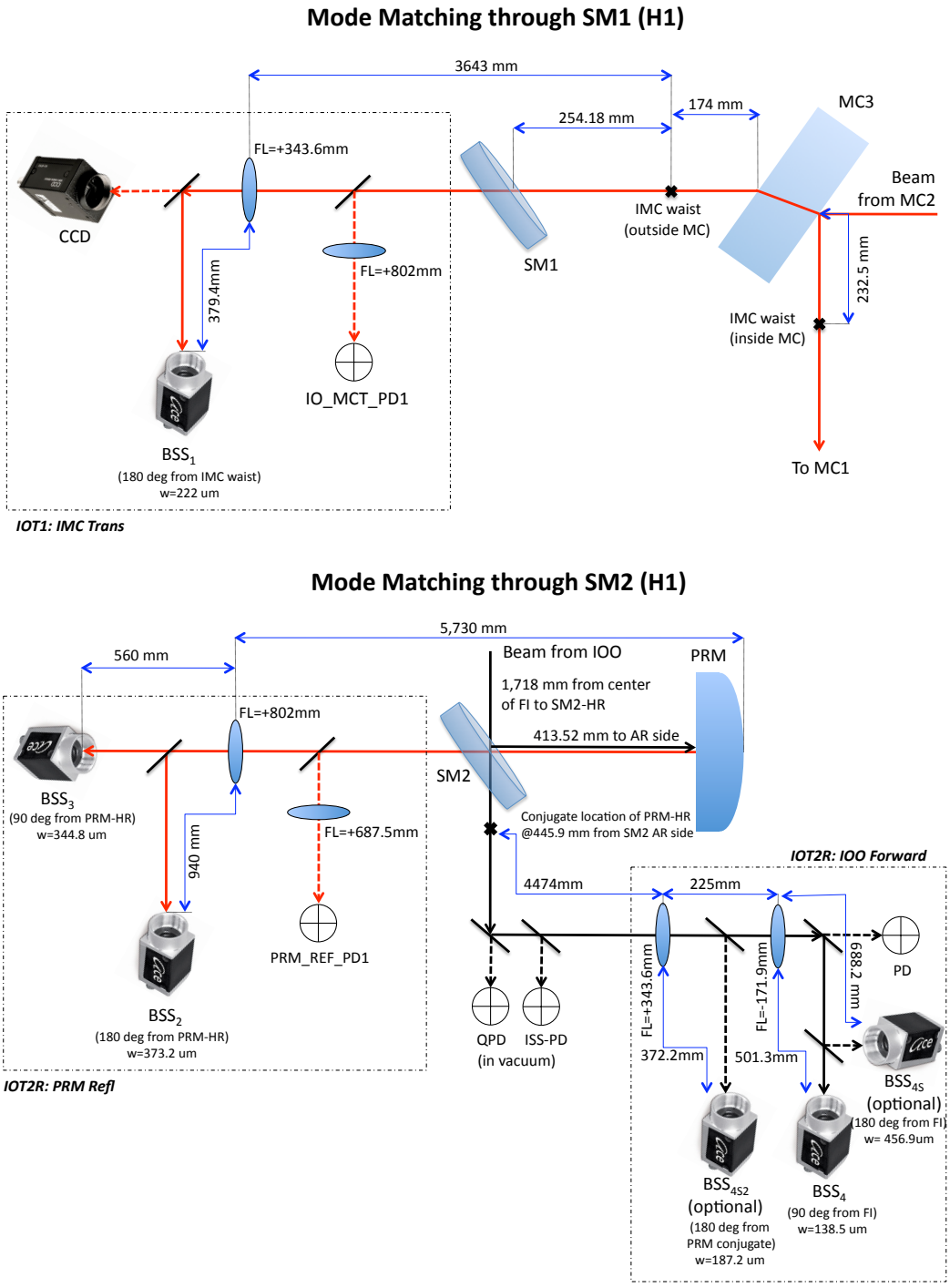

FIG. 4: IOO mode matching strategy on IOT2L and IOT2R, showing values derived using the H1 as-built parameters. Parameters for the as-built L1 are listed in Table I.

1. BSS1 Sensor

BSS1 monitors the beam size of the input mode cleaner, being placed at the virtual location of the IMC waist (180 deg Gouy phase from the waist of the IMC).

The beam parameters at the location of the BSS1 sensor are listed in Table III. The demagnification factor between IMC waist and the image size at BSS1 is constant for a specific location of the MCT-L2 lens, depending only on the ratio of the optical distances between IMC waist to MCT-L2 and MCT-L2 to BSS1. Therefore, the image from BSS1 can be well calibrated to directly monitor changes in the IMC waist size, mainly due to abnormal coating absorption.

TABLE III: Beam Parameters at BSS1

Parameter	Unit	H1	L1
IMC beam waist	mm	2.1256	2.1244
Distance IMC waist to lens MCT-L2	m	3.643	3.232
IMC waist to SM1-HR		*0.254*	*0.254*
SM1-AR to ROM RH2		*0.095*	*0.095*
ROM RH2 to IOT1 Lower Per Mirror		*2.684*	*2.684*
IOT1 Lower Per Mirror to IO-MCT-L2		*0.610*	*0.178*
Gouy phase at lens MCT-L2	deg	15.274	13.633
Focal length of lens MCT-L2	mm	343.6	687.5
Distance from lens MCT-L2 to BSS1	mm	379.4	873.3
Beam waist after lens MCT-L2	um	53.127	107.658
Distance MCT-L2 waist to BSS1	mm	33.73	179.27
Beam size at BSS1	um	221.5	574.1
Demagnification factor from IMC waist size		9.60	3.70
Current IOT2L layouts		D0902284-v10	D0902284-v10

The beam size and Gouy phase change from the IMC waist to the BSS1 sensor for H1 is shown in Figure 5.

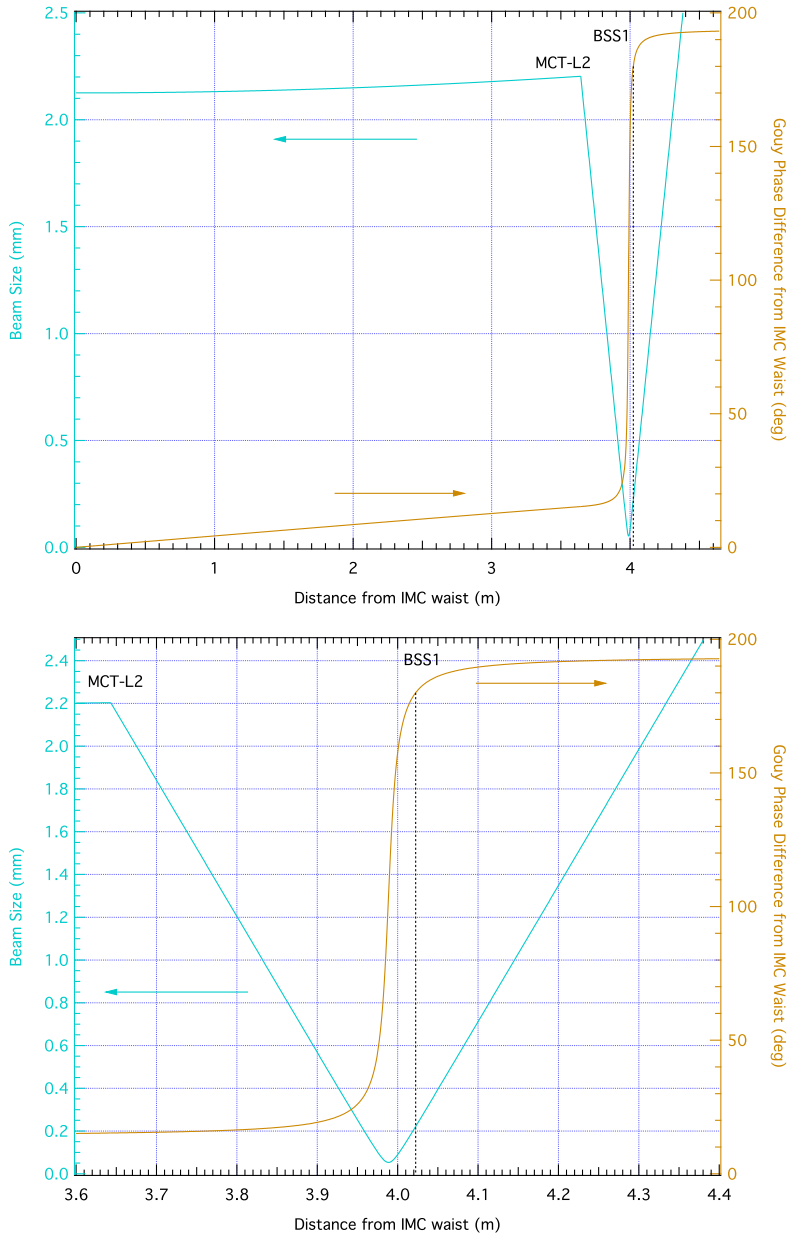

FIG. 5: Beam size and Gouy phase change from IMC waist to BSS1 derived for the H1 as-built parameters.

Similarly, Figure 6 shows the beam size and the Gouy phase change from the focusing lens IO-MCT-L2 to BSS1 for L1.

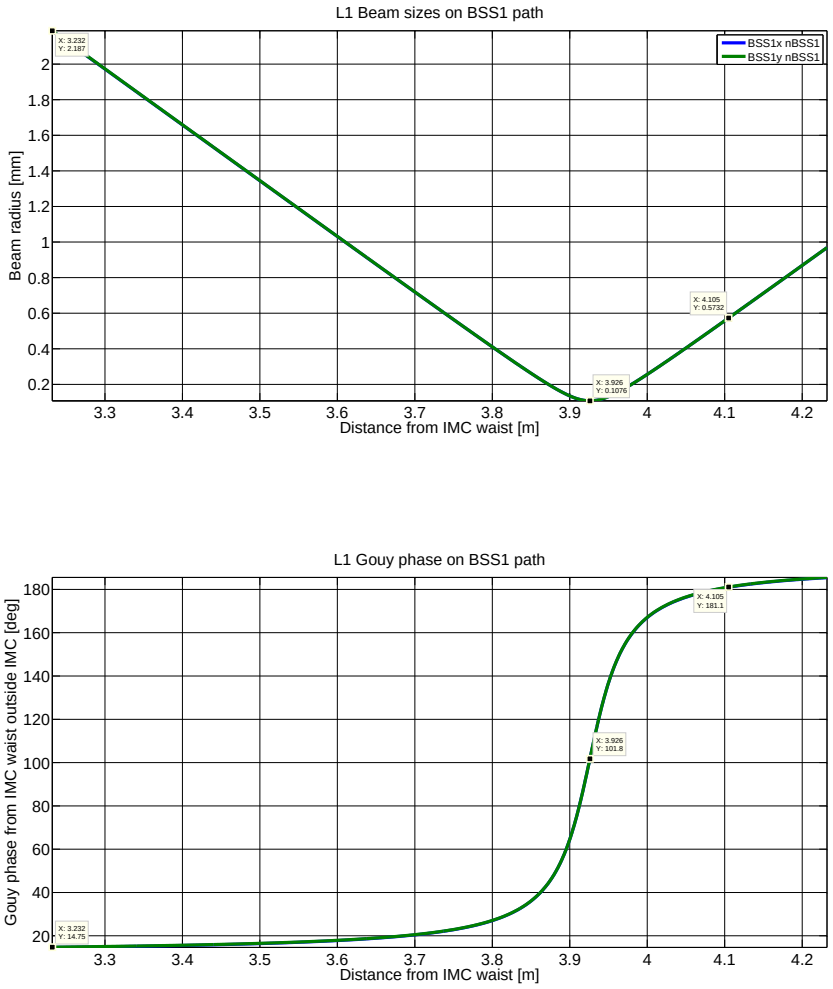

FIG. 6: Beam size and Gouy phase change from IMC waist to BSS1 derived for the current L1 as-built parameters.

The configurations for L1 and H1 to BSS1 are currently different, as the L1 path was recently modified to include a second ISS box for mode cleaner locking. As the beam size at BSS1 is now a factor of 2 larger that for H1, it is less susceptible to positioning errors and has better sensitivity to IMC beam waist change. If beam clipping at BSS1 is not an issue (the sensor size is 3.69 mm x 2.77 mm, which is only a factor of 2.4 larger than the beam diameter on y-axis), we can follow the same modifications at LHO.

The sensitivity of the beam size at the BSS1 sensor to the IMC waist size and to the positioning of this sensor is shown in Figures 7 - 9.

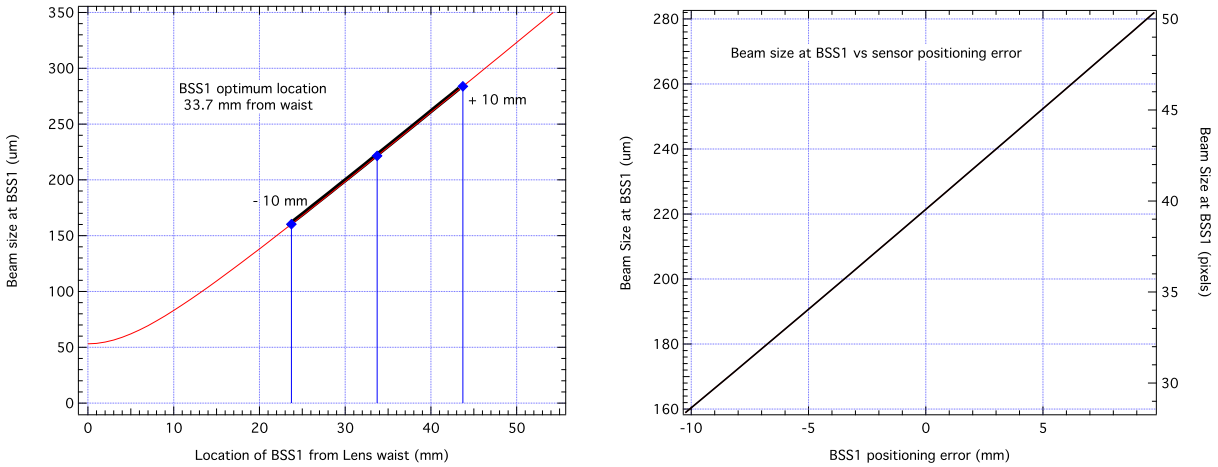

FIG. 7: Beam size change at BSS1 as function of positioning from IO-MCT-L2 for H1.

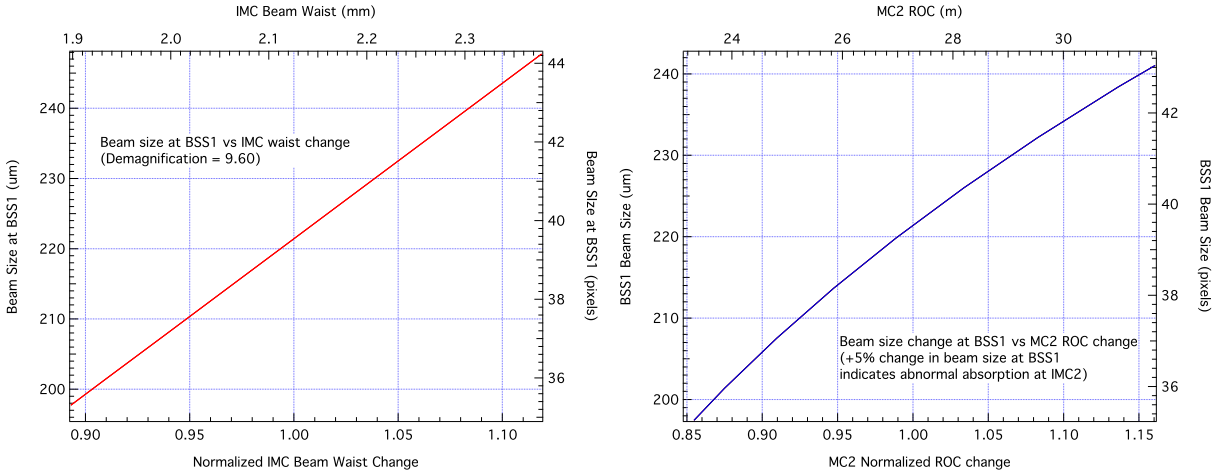

FIG. 8: Beam size change at BSS1 as function of the IMC waist and MC2 ROC change for H1.

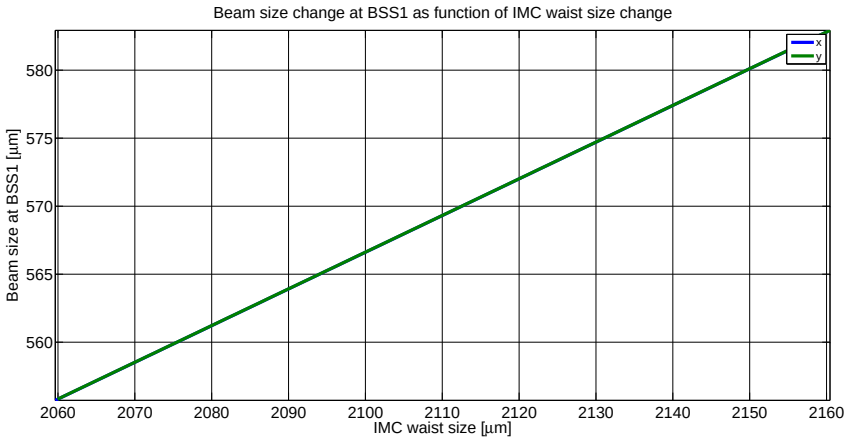

FIG. 9: Beam size change at BSS1 as function of the IMC waist change for L1.

As the Rayleigh range after IO-MCT-L2 is very short ($\sim$ 8 mm), errors in its location will drastically affect the measured beam size. The fine alignment and positioning of this sensor should therefore be done following T1300617, by measuring the beam profile after this lens, and determining the actual Gouy phase change from the waist.

To measure the IMC beam size with 5% accuracy, BSS1 should be positioned within 1 mm from its optimum position (for H1). However, relative changes can be measured much more accurately, as they only depend on the pixel size and the sensitivity of the GigE camera.

2. BSS5 Sensor

This sensor samples the MC REFL beam on the path to the wavefront sensors for the ALS alignment. It does not have a strictly defined location, as it is used to only qualitatively observe the mode mismatching into the mode cleaner from the PSL. It can be set up to track down relative changes in the beam profile and visualize the higher order mode content into IMC at imperfect alignment and mode matching.

V. MODE MATCHING ON IOT2R (IOT2)

There is a total of 5 beam sensors on IOT2R, designated to monitor and diagnose the parameters of the beams exiting HAM2 through the SM2 (IM4) mirror. Of these, only BSS2, BSS3 and BSS4 are designed for continuos monitoring, while BSS4s and BSS4s2 are spares used on limited durations for tests and measurements during commissioning periods.

The evolution of the beam from the waist of the IMC to these sensors on IOT2R is shown in Figure 10.

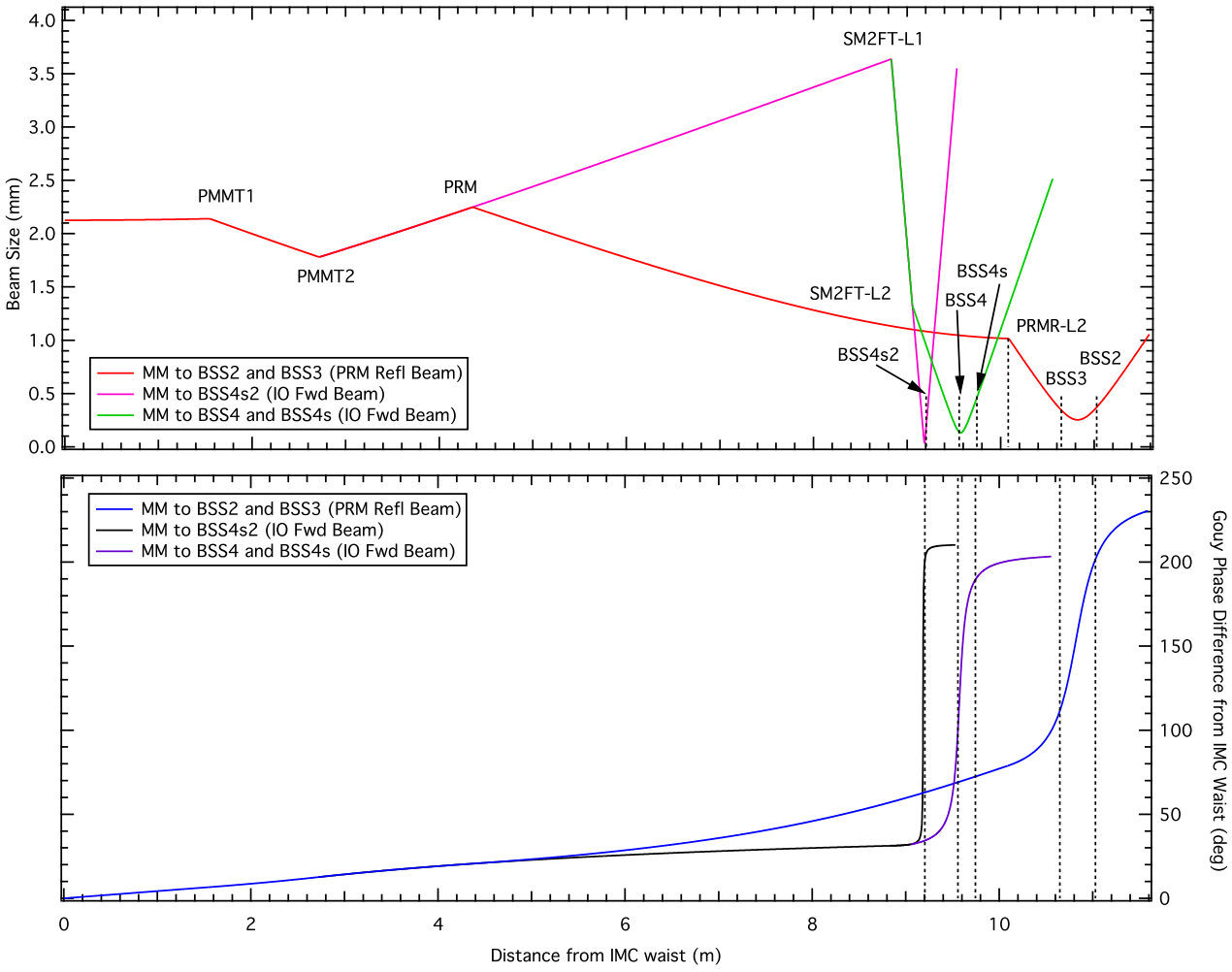

FIG. 10: Beam size and Gouy phase change from the waist of the mode cleaner to the BSS on IOT2R. See Figures 11, 14 and 17 for expanded views.

3. BSS2 and BSS3 Sensors

These sensors are placed in the beam reflected off the power recycling mirror and transmitted back through SM2 and then routed to IOT2R. They are positioned at 90 deg (BSS3) and 180 deg (BSS2) Gouy phase from the HR side of PRM. The BSS2 sensor is therefore placed at the conjugate location of PRM, allowing us to directly monitor changes in the beam size at PRM. Once this sensor is positioned properly, absolute calibration is possible if the distances from PRM to BSS2 are known accurately.

The beam size and the Gouy phase change from the conjugate location of PRM to the BSS2 and BSS3 sensors is shown in Figure 11, and the main parameters are summarized in Table IV.

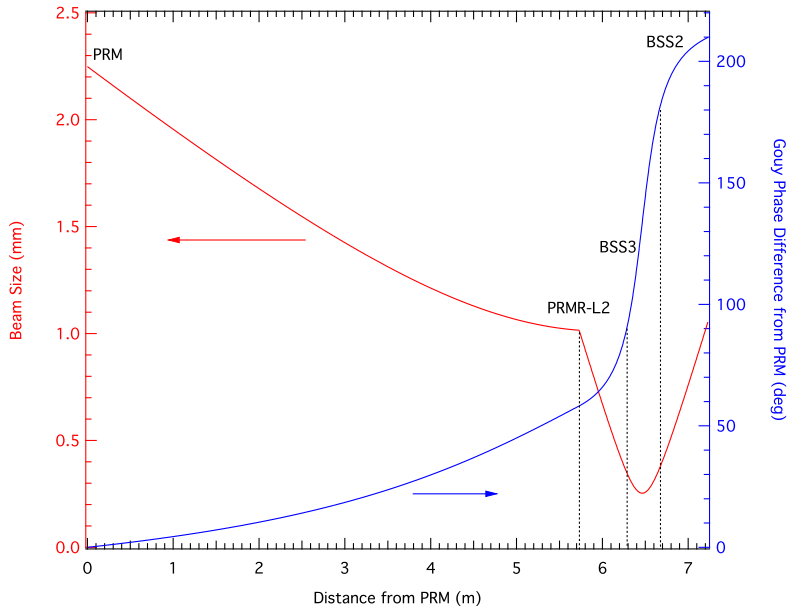

FIG. 11: Evolution of the beam size and accumulated Gouy phase to BSS2,3 sensors from PRM. These values are derived using the H1 as-built parameters.

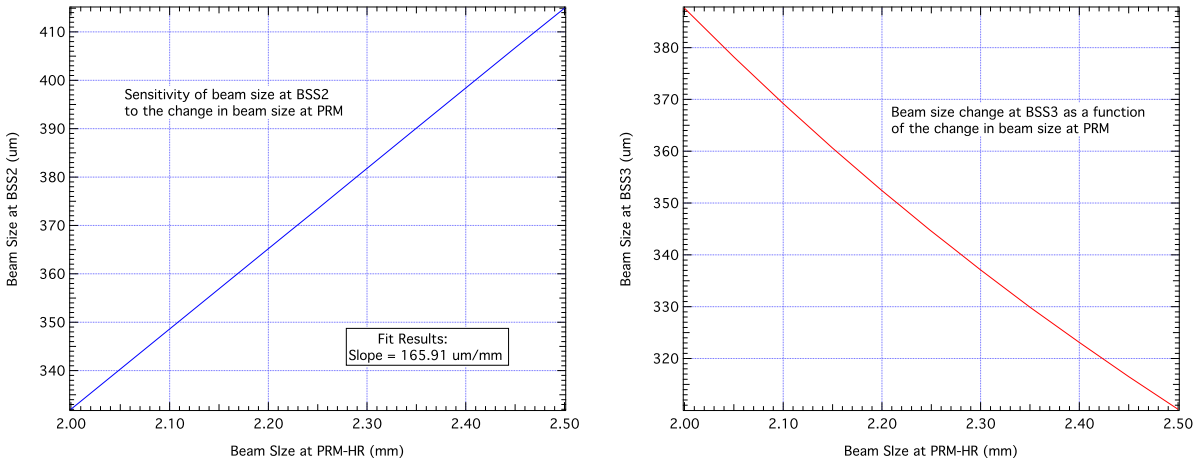

FIG. 12: Beam size change at the BSS2 and BSS3 sensors as a function of the beam size change at PRM. These values are derived using the H1 as-built parameters.

Figure 12 shows the beam size change at BSS2 and BSS3 sensors as a function of the beam size at PRM. As the demagnification at BSS3 is constant for a specific location of the IO-PRM-L2 lens (depending only on the optical distances between PRM to IO-PRM-L2 and IO-PRM-L2 to BSS3) it could be convenient to calibrate the camera from the software to show directly the size of the

beam at PRM.

In Figure 13 we plotted the sensitivity of these to sensors to changes in the PRM radius of curvature. As expected, the sensitivity of the beam size measured at BSS2 (90 deg Gouy phase

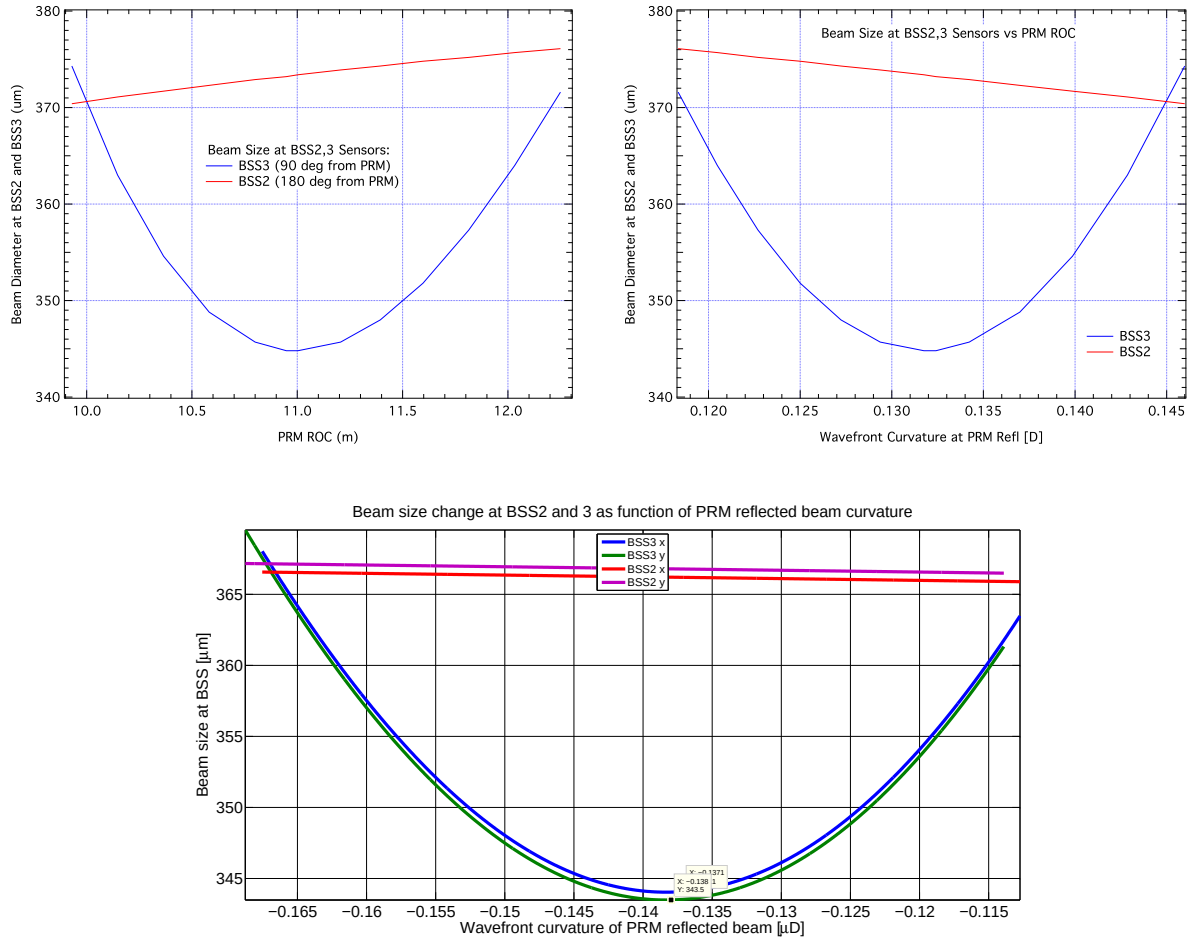

FIG. 13: Beam size change at the BSS2 and BSS3 sensors as a function of the ROC change at PRM. Derived using as-built H1 (top) and L1 (bottom) data.

from PRM) is negligible compared to measurements at BSS3 (180 deg Gouy phase from PRM). However, close to the nominal ROC value, the slope is very flat for BSS3.

TABLE IV: Beam Parameters at BSS2 and BSS3

Parameter	Unit	H1	L1
Beam waist after reflection off PRM	mm	1.0114*	1.0203*
Beam size at PRM-HR	mm	2.2485	2.2489
Distance PRM-HR to lens PRM-L2	m	5.730	5.734
PRM-AR to SM2-HR		*0.414*	*0.418*
SM1-AR to ROM LH2		*0.192*	*0.192*
ROM LH2 to ROM RH6		*0.663*	*0.663*
ROM RH6 to Viewport		*1.262*	*1.262*
Viewport to IOT2R Lower Per Mirror		*1.510*	*1.510*
IOT2R Lower Per Mirror to IO-MCR-L2		*1.619*	*1.619*
Gouy phase change from PRM to PRM-L2	deg	58.17	57.39
Focal length of lens PRM-L2	mm	802	802
Beam waist after lens PRM-L2	um	253.11	250.52
Distance from lens PRM-L2 to BSS3	mm	560	561
Distance from lens PRM-L2 to BSS2	mm	940	932
Distance PRM-L2 waist to BSS2	mm	205	197
Beam size at BSS3	um	344.8	344.0
Beam size at BSS2	um	373.2	365.6
Demagnification factor at BSS2 from PRM beam size		6.04	6.15
*This is probably because of the mode mismatch between the beam and the ROC of PRM w0=1.0187 mm (H1) and w0=1.0186 mm (L1) for the beam incident on PRM			

4. BSS4, BSS4s and BSS4s2 Sensors

These sensors are placed in the IO forward beam, to monitor the beam profile and detect changes in the beam size due to thermal effects in the Input Optics, mostly the Faraday isolator.

BSS4 is at 90 deg Gouy phase from the center of the Faraday isolator, to indirectly determine thermal effects in the far field. BSS4s is used occasionally during commissioning or testing to monitor the beam size inside the Faraday isolator, as it is placed at the conjugate location from the center of FI - 180 deg Gouy phase from it.

BSS4s2 is another sensor used infrequently during testing and commissioning, and it images the conjugate location of the PRM in the forward direction transmitted through SM2. It is located 180 deg Gouy phase from this location. The image from this sensor can be compared to the one from BSS2 and, with proper calibration, the mode matching into the interferometer can be optimized

by minimizing the discrepancies between the images provided by these two sensors.

The beam size and the Gouy phase change from the Faraday isolator to the BSS4 and BSS4s is shown in Figure 14, and the main parameters are summarized in Table V.

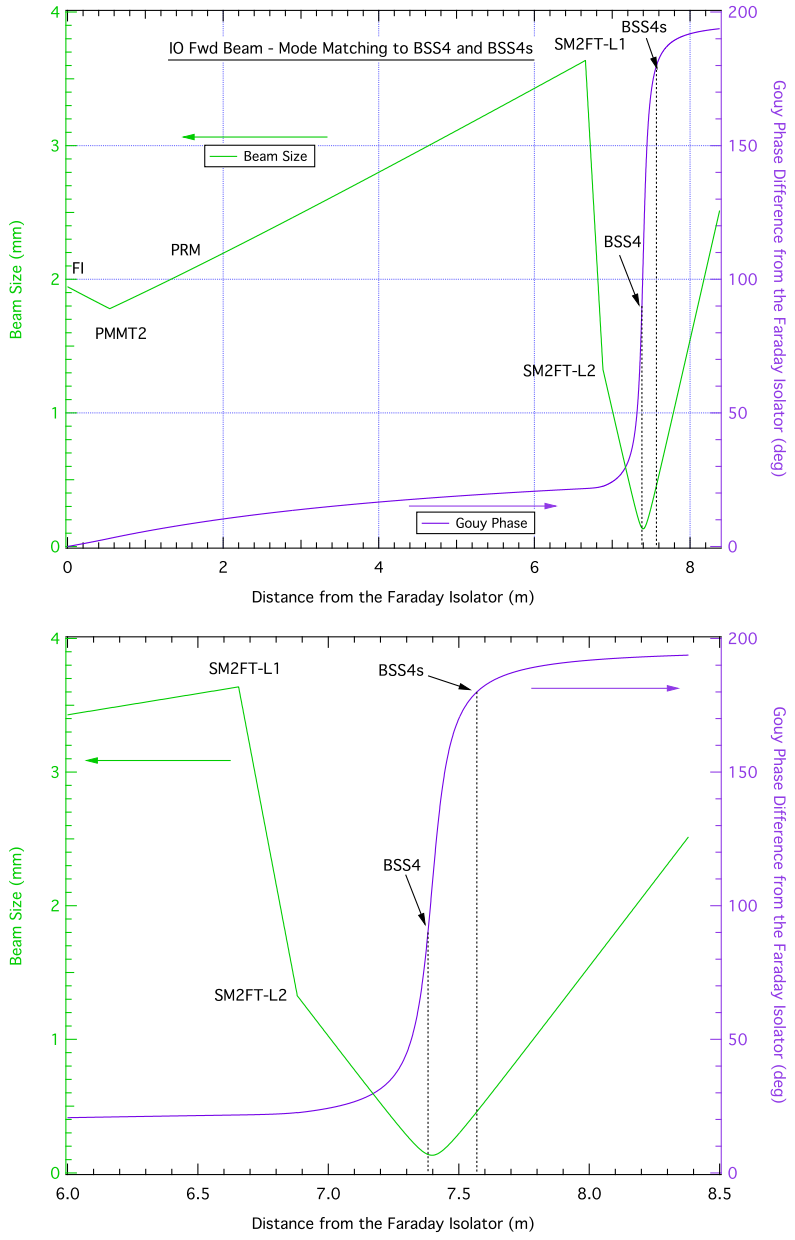

FIG. 14: Evolution of the beam size and accumulated Gouy phase to BSS4,4s sensors from the Faraday isolator. These values are derived using the H1 as-built parameters.

Figure 15 shows the beam size change at the BSS4 and BSS4s sensors as a function of the beam size and inverse focal length at the center of the Faraday isolator.

IO is required to provide 95% of the TEM00 mode content into the interferometer. The effect

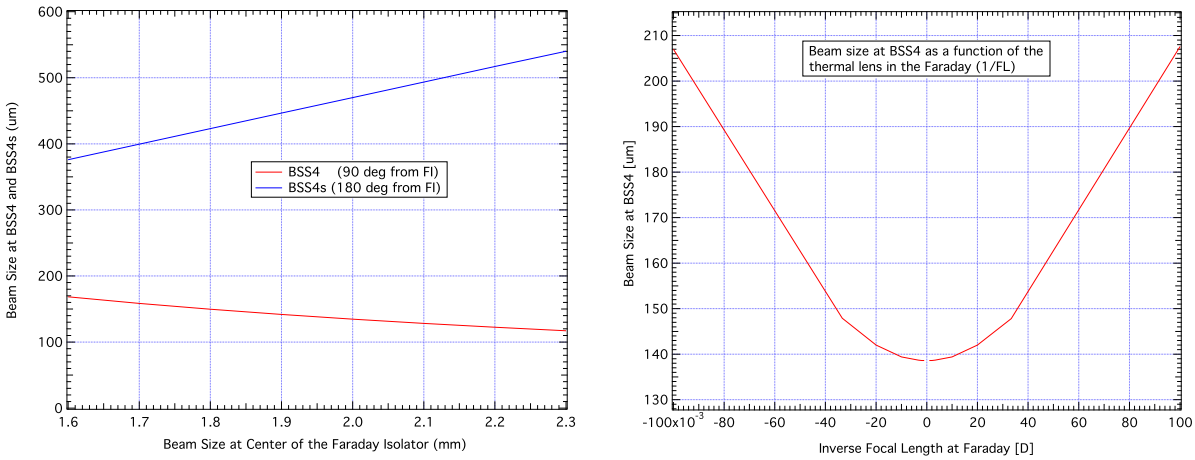

FIG. 15: Beam size change at BSS4 and BSS4s as a function of the beam size change (a) and of the thermal lens (b) at the center of the Faraday isolator. The beam size change at BSS4s is not affected by the thermal lens in the Faraday

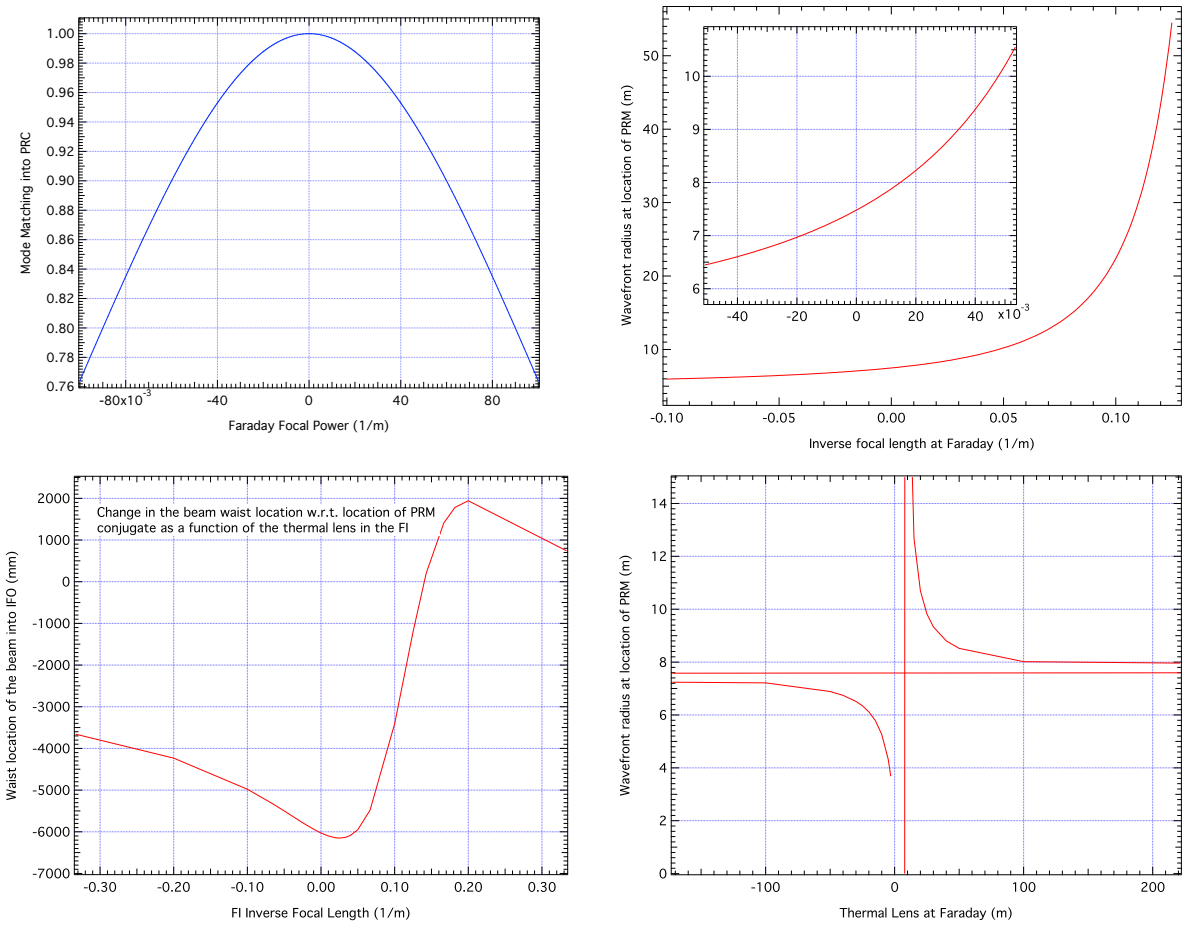

FIG. 16: Effect of the thermal lensing in the Faraday isolator on the mode matching into the interferometer and on various parameters affecting it.

of the thermal lensing in the Faraday on the mode matching is shown in Figure 16 top left graph, and we can see that the maximum allowed focal power to meet this requirement is 0.040 m^{-1} or a focal length of 25 m. This translates into a maximum beam size at BSS4 of 155 um. This assumes that beam profile measurements agree with the theoretical values and the sensor was positioned properly. For alignment see T1300617. Figure 16 also shows the effect of the Faraday thermal lensing on the wavefront radius at PRM (top and bottom right) and the location of the beam waist into the IFO from the location of PRM-HR (bottom left).

TABLE V: Beam Parameters at BSS4 and BSS4s

Parameter	Unit	H1	L1
Beam size at center of Faraday isolator	mm	1.9441	1.9431
Gouy phase change from IMC waist to FI	deg	9.547	9.558
Beam waist after SM2	mm	1.01868	1.018623
Distance center of FI to lens SM2FT-L1	m	6.656	6.656
FI center to SM2-HR		*1.718*	*1.718*
SM2-AR to ROM LH1		*0.100*	*0.100*
ROM LH1 to ROM RH3		*0.644*	*0.644*
ROM RH3 to ROM RH4		*0.055*	*0.055*
ROM RH4 to ROM RH5		*0.620*	*0.620*
ROM RH6 to Viewport		*1.262*	*1.262*
Viewport to IOT2R Lower Per Mirror		*1.510*	*1.510*
IOT2R Lower Per Mirror to IO-SM2FT-L1		*0.728*	*0.728*
Gouy phase change from FI to SM2FT-L1	deg	21.698	21.716
Focal length of lens SM2FT-L1	mm	343.6	343.6
Beam waist after lens SM2FT-L1	um	32.986	32.994
Distance between lenses SM2FT-L1 and SMTFT-L2	mm	225	225
Gouy phase change from SM2FT-L1 to SM2FT-L2	deg	0.904	0.905
Focal length of lens SM2FT-L2	mm	-171.9	-171.9
Beam waist after lens SM2FT-L2	um	132.582	132.6234
Beam waist location after SM2FT-L2	mm	517.1 mm	517
Distance from lens SM2FT-L2 to BSS4	mm	501.3	501.35
Distance from lens SM2FT-L2 to BSS4s	mm	688.2	688.3
Distance SM2FT-L2 waist to BSS4s	mm	171.1	171.1
Beam size at BSS4 *(90 deg from center of FI)*	um	138.5	138.6
Beam size at BSS4s *(180 deg from center of FI)*	um	456.9	456.7
Demagnification factor at BSS4s from FI beam size		4.26	4.24

The beam size and the Gouy phase change from the conjugate location to BSS4s2 is shown in Figure 17, and the main parameters are summarized in Table VI.

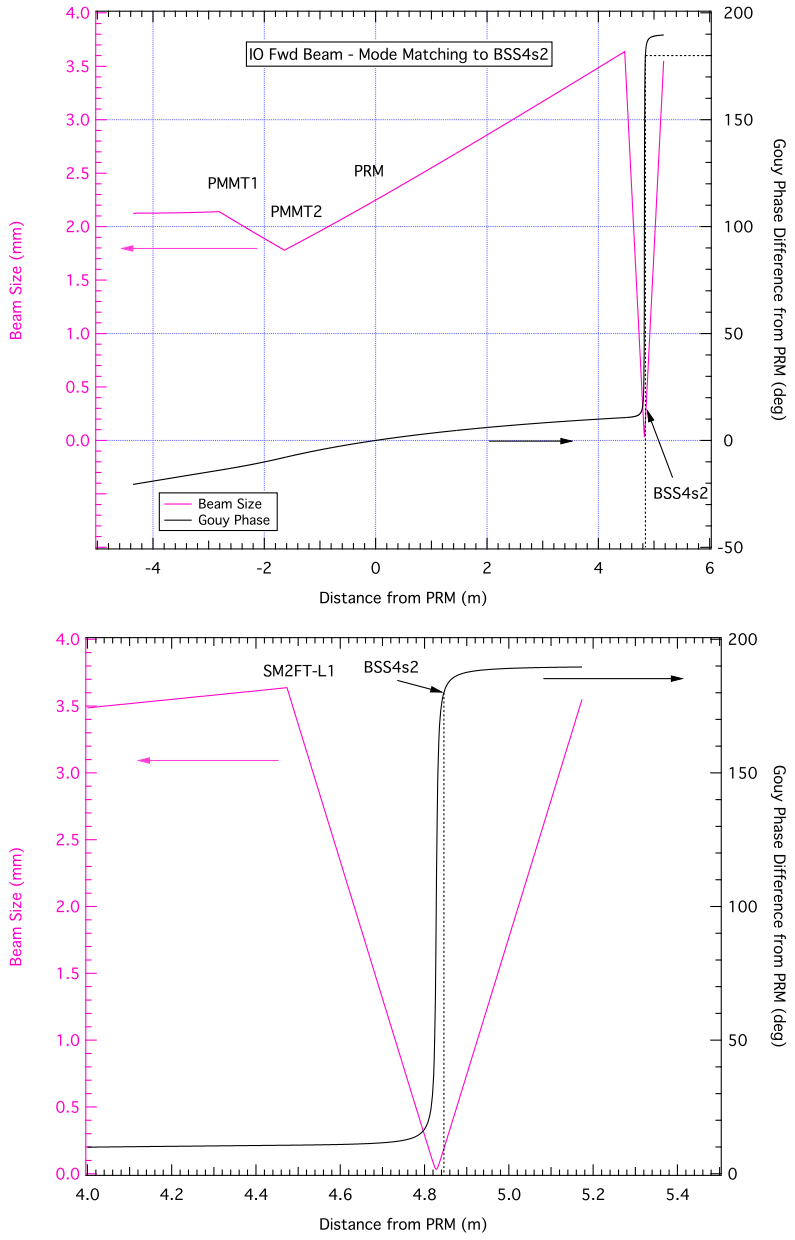

FIG. 17: Evolution of the beam size and accumulated Gouy phase to BSS4s2 sensors from PRM. These values are derived using the H1 as-built parameters.

Figure 18 shows the beam size change at BSS4s2 as a function of beam size change at PRM, and as a function of the positioning errors of the sensor. As the Rayleigh range after IO-SM2FT-L1 is very short, $\pm$ 3 mm errors in its location will cause changes of $\sim$ 15% in the measured beam size. The fine alignment and positioning of this sensor should therefore be done following T1300617, by

measuring the beam profile after this lens, and determining the actual Gouy phase change from the waist.

Calibration between beam size measurements at the sensors BSS2 and BSS4s2 is shown in Figure 19.

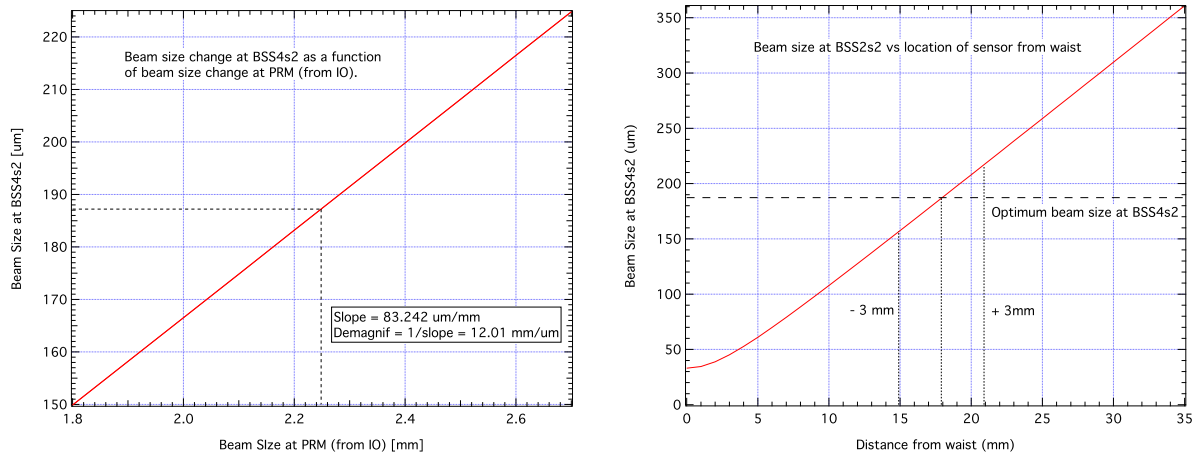

(a) (b)

FIG. 18: Beam size change at BSS4s2 as a function of beam size change at PRM (a) and as a function of the positioning errors of the sensor (b).

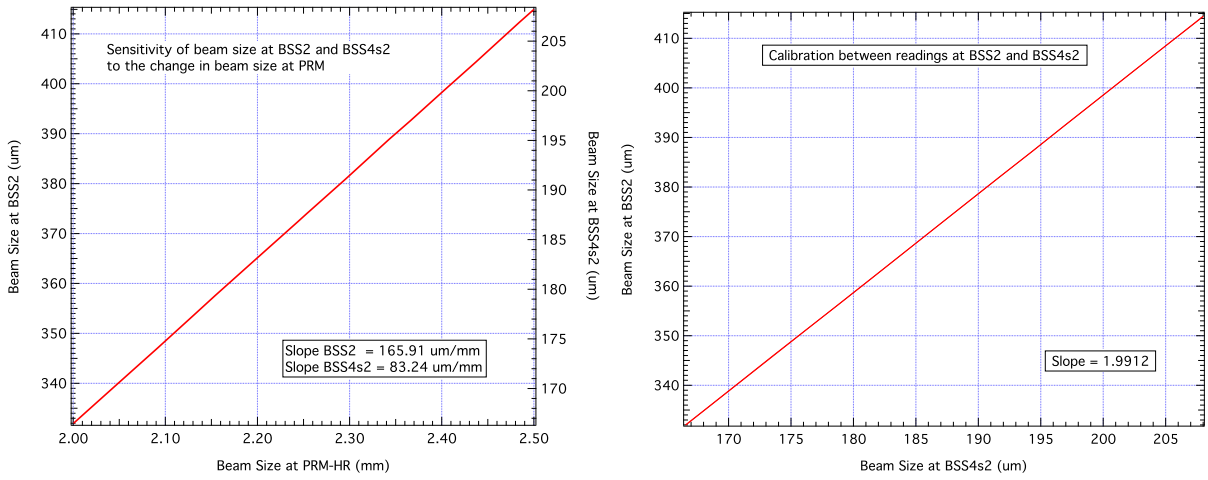

FIG. 19: Relationship between beam size readings at sensors BSS2 and BSS4s2.

The effect of Faraday thermal lensing on the beam size measured at BSS4s2 is shown in Figure 20.

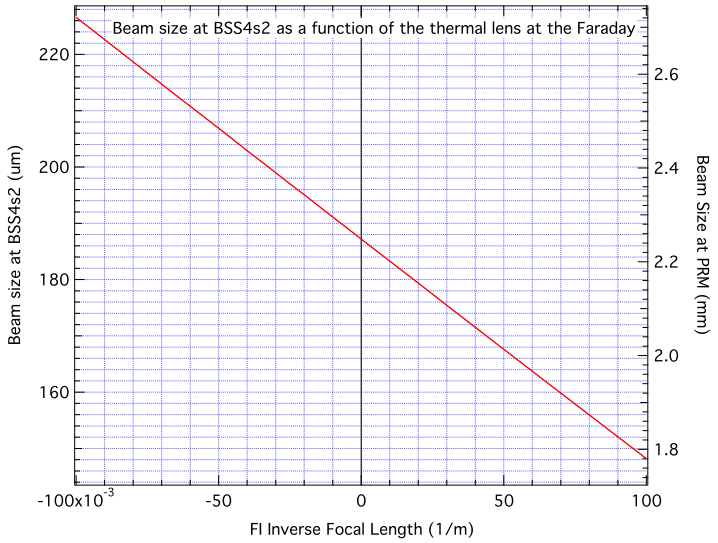

FIG. 20: Effect of the thermal lensing in the Faraday isolator on the reading at BSS4s2.

TABLE VI: Beam Parameters at BSS4s2

Parameter	Unit	H1	L1
Beam waist after SM2	mm	1.01868	1.018626
Conjugate location of PRM-HR from SM2-AR	mm	445.87	450.35
Beam size at PRM conj.	mm	2.2485	2.2489
Gouy phase change from IMC to PRM conj.	deg	20.570	20.608
Distance SM2-AR to lens SM2FT-L1	m	4.919	4.919
SM2-AR to ROM LH1		*0.100*	*0.100*
ROM LH1 to ROM RH3		*0.644*	*0.644*
ROM RH3 to ROM RH4		*0.055*	*0.055*
ROM RH4 to ROM RH5		*0.620*	*0.620*
ROM RH6 to Viewport		*1.262*	*1.262*
Viewport to IOT2R Lower Per Mirror		*1.510*	*1.510*
IOT2R Lower Per Mirror to IO-SM2FT-L1		*0.728*	*0.728*
Gouy phase change from PRM conj. to SM2FT-L1	deg	10.676	10.673
Focal length of lens SM2FT-L1	mm	343.6	343.6
Beam waist after lens SM2FT-L1	um	32.986	32.994
Beam waist location after SM2FT-L1	mm	354.3	354.3
Location of SM2FT-L1 waist from BSS4s2	mm	372.2	372.2
Distance SM2FT-L1 waist to BSS4s2	mm	17.9	17.9
Beam size at BSS4s2	um	187.2	187.3
Demagnification factor at BSS4s from PRM beam size		12.01	12.01

VI. CONCLUSIONS

Within the software, the data from the BSS1, BSS2, BSS4s and BSS4s2 GigE cameras could be conveniently displayed directly as beam sizes using the scale factors provided in the corresponding tables. These scale factors should first be confirmed during the initial calibration of the sensors, when all the distances are well known, and the routines for beam analysis have been thoroughly evaluated.

The scaled beam size difference between BSS2 and BSS4s2 can be used to improve mode matching from IO into the PRC.

For rigorous positioning of the sensors, it is necessary to measure the beam profile and calculate the Gouy phase difference from the particular waist, according to the alignment document T1300617.